Iron-impregnated granular activated carbon for arsenic removal: Application to practical column filters

Mahatheva Kalaruban[1], Paripurnanda Loganathan[1], Tien Vinh Nguyen[1], Tanjina Nur[1], Md Abu Hasan Johir[1], Thi Hai Nguyen[2], Minh Viet Trinh[2], Saravanamuthu Vigneswaran[1]*

[1]Faculty of Engineering and Information Technology, University of Technology, Sydney, NSW, 2007, Australia

[2]Institute of Environmental Technology, Vietnam Academy of Science and Technology, 18 Hoang Quoc Viet Road, Hanoi, Viet Nam

*corresponding author: s.vigneswaran@uts.edu.au

Tel: 61 – 2 – 9514 2641

Fax: 61 – 2- 9514 2633

Highlights

- Incorporating Fe into granular activated carbon (GAC) increased As(V) adsorption.
- GAC-Fe's higher As removal is due to more positive charges and specific adsorption.
- Intra-particle diffusion processes controlled adsorption kinetics
- GAC-Fe treated more water than GAC in reducing As levels to WHO guideline level.

Abstract

Arsenic is a major drinking water contaminant in many countries causing serious health hazards, and therefore, attempts are being made to remove it so that people have safe drinking water supplies. The effectiveness of arsenic removal from As(V) solutions using granular activated carbon (GAC) (zero point of charge (ZPC) pH 3.2) and iron incorporated GAC (GAC-Fe) (ZPC pH 8.0) was studied at 25 ± 1^{o}C. The batch study confirmed that GAC-Fe had higher Langmuir adsorption capacity at pH 6 (1.43 mg As/g) than GAC (1.01 mg As/g). Adsorption data of GAC-Fe fitted the Freundlich model better than the Langmuir model, thus indicating the presence of heterogeneous adsorption sites. Weber and Morris plots of the kinetic adsorption data suggested intra-particle diffusion into meso and micro pores in GAC. The column adsorption study revealed that 2-4 times larger water volumes can be treated by GAC-Fe than GAC, reducing the arsenic concentration from 100 µg/L to the WHO guideline of 10 µg/L. The volume of water treated increased with a decrease in flow velocity and influent arsenic concentration. The study indicates the high potential of GAC-Fe to remove arsenic from contaminated drinking waters in practical column filters.

Keywords: arsenic, adsorption, adsorption models, granular activated carbon, water treatment

1. Introduction

Arsenic (As)-contaminated drinking water is one of the main causes of As toxicity in several countries such as Bangladesh, parts of India, Vietnam, and Cambodia. Arsenic-induced skin lesions have been reported among people in these countries. The groundwater As concentration is as high as 3.05 mg/L in Vietnam (Luu

2017) and 0.6 mg/L in Bangladesh (Meng et al. 2001). To protect people from As toxicity, regulatory agencies in many countries have set maximum limits (0.01-0.05 mg/L) for As in drinking water (Mondal and Garg 2017). The US Environmental Protection Agency (USEPA), Health Canada, and European Union (EU) have an As concentration limit of 0.01 mg/L in drinking water. The same concentration is recommended as a guideline by the World Health Organization (WHO). Due to the toxic effects of As, there are much scientific interests in developing appropriate technologies for the removal of As from drinking water sources.

Groundwater containing As can be remediated by various methods such as precipitation, coagulation, ion exchange, membrane techniques, and adsorption (Kabir and Chowdhury 2017, Mohanty 2017). Of these processes, adsorption is the most cost-effective, simple, and efficient one as it can even remove tiny amounts of As from water, and for this reason, it has been widely used (Mondal and Garg 2017). Furthermore, the process produces minimum chemical or biological sludge and the adsorbent can be regenerated and reused thereby curtailing the costs of this process (Loganathan et al. 2014, Mohanty 2017). In the adsorption process, As is removed by electrostatic attraction or coulombic forces (outer-sphere complexation) on adsorbents such as ion exchange resins and by specific adsorption, ligand exchange or H bonding (inner-sphere complexation) on adsorbents such as iron oxide (Loganathan et al. 2014, Mohanty 2017).

Arsenic toxicity is prevalent mainly in developing countries. Therefore, low-cost locally available adsorbents are more appropriate and affordable to the people at the village level in these countries. Of the various low-cost absorbents, activated carbon (AC) made from locally available agricultural wastes has been proven to be one of the most popular and reliable adsorbents used for removing As, probably due to its high

surface area and porous structure (Chuang et al. 2005, Gu et al. 2005, Loderio et al. 2013, Manju et al. 1998, Natale et al. 2008). Furthermore, it is universally used to remove numerous organic and inorganic pollutants in water (Mohanty 2017) and therefore when utilised for As removal, the other pollutants in water can also be removed simultaneously. However, the adsorption capacity of AC for As is low. To increase the adsorption capacity, in some studies the AC has been modified by incorporation of iron (Fe) oxide/hydroxide (Tuna et al. 2013, Chang et al. 2010, Liu et al. 2010) and zirconium (Zr) salts (Daus et al. 2004). Furthermore, incorporating metal onto the AC, especially the granular AC (GAC), provides a more practical means of taking advantage of the beneficial outcome of metal in removing As. GAC provides a skeletal strength to the metal oxide/hydroxides, as compared to the relatively fragile nature of the metal oxide/hydroxides media if they are used alone as an adsorbent, especially in the column-based adsorption process. Furthermore, the metal oxides/hydroxides might create more effective adsorption sites within a porous AC support media. This is important because the column-based fixed bed process is practical and commonly used in water treatment plants throughout the world.

At the village level, sand filtration is commonly being used in many countries such as Vietnam and Bangladesh where the Fe concentration in groundwater is high (Berg et al. 2006; Meng et al. 2001; Nguyen et al. 2009). Here, the dissolved Fe^{2+} forms coatings on the sand as hydroxides after being oxidised to Fe^{3+}, which thereby increases the adsorption of As (Berg et al. 2006). Although ≥ 90% of As has been removed employing this system, the As concentrations in many of the filtered water bodies were higher than the WHO guideline concentration (Nguyen et al. 2009). For this reason, a more efficient adsorbent than sand such as GAC or metal oxide impregnated GAC is required to reduce the As concentration further.

Many studies have been conducted on the use of various types of AC for the removal of As, but most of them used static batch experiments (Mondal and Garg 2017). Only a limited number of studies have been conducted in dynamic column-mode experiments which are more applicable to the practical operating system. Daus et al. (2004) reported one such study using Zr incorporated AC but at only one As concentration and one flow velocity.

The aims of this study were to: firstly, measure the kinetics and equilibrium adsorption of As by a Fe incorporated GAC (Fe-GAC) in batch and column experiments using realistic As concentrations; and secondly. determine the volume of water that can be treated with Fe-GAC in column experiments at different As concentrations and flow velocities to bring the As concentrations below the WHO guidelines concentration. The novelty of the study is to compare the As adsorption performance of the commonly used GAC adsorbent in practical dynamic water treatment process with Fe-GAC in both batch and column-based experiments. Column-based studies which have direct relevance to practical plant operations have rarely been reported previously for Fe-GAC. Also, the effect of flow velocity and initial As concentration on As removal by Fe-GAC, which have practical significance, appears to have not been reported previously.

2. Materials and methods

2.1. Materials

GAC (0.3–2.4 mm) was supplied by James Cummins P/L, Australia. A narrow particle size range of 300-600 µm was separated by sieving the original material, and the sieved material was used for the study. Using such a narrow particle size was expected to reduce the experimental variability. GAC-Fe was prepared by mixing 20 g GAC with 500 mL 0.1 M $FeCl_2$ obtained from Sigma-Aldrich (USA) inside an Erlenmeyer flask and adjusting the pH to 4.2-4.5 (Gu et al. 2005). The flask was then agitated in a flat shaker at 150 rpm for 24 h at a room temperature of 25 ± 1 ^{o}C. The suspension was filtered and the residue was washed many times with de-ionised water to remove any Fe salts and colloidal precipitates adhering to the external surface of the GAC-Fe material before drying at room temperature for 24 h.

2.2. BET surface area, porosity and scanning electron microscopy

The GAC and GAC-Fe samples were degassed at 150 °C for 13 h under vacuum before the surface area and porosity measurements. The Brunauer-Emmett-Teller (BET) method was used to determine the surface area by N_2 adsorption isotherms at 77 K using Autosorb iQ-C. The Barrett-Joyner-Hanlenda (BJH) method served to calculate the total pore volume and average pore diameter. The samples' surface morphology was determined with a Hitachi S3400 scanning electron microscope which was operated at 20 kV. Duplicate samples were used for the analyses.

2.3. Chemical analysis of adsorbents

The ash content of GAC was determined by heating 1 g GAC in an oven set at 700 ^{o}C for 18 h and measuring the weight loss. The percentage of Fe in the Fe-GAC was determined by dissolving triplicate subsamples of 0.1 g Fe-GAC sample in 100 mL 1:1 HCl solution in a flask. The suspension was stirred for 4 h and filtered. The Fe concentration in the filtrate was measured with a Microwave Plasma - Atomic Emission Spectroscopy (MP-AES) (Agilent 4100).

2.4. Zeta potential

The zeta potential was determined on 1.0 g/L of GAC and GAC-Fe suspensions in the presence of 10^{-3} M of NaCl at pH ranging from 2.5 to 10.0 in the presence and absence of As with a Zetasizer nano instrument (Nano ZS Zen3600, Malvern, UK). As concentration used was 100 µg/L. The suspensions at the different pHs were agitated in a shaker for 18 h and triplicate zeta potential measurements were done on each sample. The initial pH and the final pH were also measured using a pH meter.

2.5. Batch adsorption experiments

A series of glass flasks containing 100 mL solutions of 100 µg/L As(V) at pH 6.0 and adsorbent doses ranging from 0.1 to 0.8 g/L were agitated in a shaker at 120 rpm for 24 h at 25 ± 1 ^{o}C. Analar-grade sodium arsenate dibasic heptahydrate ($Na_2HAsO_4.7H_2O$) obtained from Sigma-Aldrich (Australia) was used to prepare the As(V) solutions. The suspensions' pH was checked after 4 h of agitation and found to have increased from the initial value of 6.0 probably due to ligand exchange of As with the OH groups on the adsorbent surface. Therefore, the pH was adjusted back to their initial value using 0.1 M HCl, and the agitation continued. The final pH values at the end of the shaking period remained at approximately 6.0. A portable pH Meter (HQ40d, HACH) was used for all pH measurements. The suspensions were then filtered and

the filtrates were analysed for As using an ICP-MS analyser. Commercial As standard for ICP-MS, TraceCERT® of 1 mg/L As concentration in nitric acid (1 mg/L As in 2% nitric acid, prepared using high purity As_2O_3) was used in the analysis. This standard was obtained from Sigma-Aldrich (Australia). The amount of As adsorption at equilibrium, q_e (µg/g), was calculated using the equation given below:

$$q_e = \frac{(C_0 - C_e).V}{m} \qquad [1]$$

where C_0 is initial concentration of As (µg /L), C_e is equilibrium concentration of As (µg /L), V is volume of solution (L), and m is mass of adsorbent (g). Percentage adsorption was calculated using the equation written as follows:

$$\text{Percentage adsorption (\%)} = \frac{(C_0 - C_e)}{C_0} \times 100 \qquad [2]$$

The data was modelled using Langmuir (equation 3) and Freundlich (equation 4) adsorption isotherms.

$$q_e = \frac{q_m K_L C_e}{1 + K_L C_e} \qquad [3]$$

where C_e = equilibrium concentration of As (µg/L), q_e = amount of As adsorbed per unit mass of adsorbent (µg/g), q_m = maximum amount of As adsorbed per unit mass of adsorbent (µg/g), K_L = Langmuir constant (L/µg) relating to the energy of adsorption.

$$q_e = K_f C_e^{1/n} \qquad [4]$$

where K_F= Freundlich constant (mg/g) $(L/\mu g)^{1/n}$, n = Freundlich constant, q_e = the amount adsorbed per unit dosage of the adsorbent (µg/g).

The change of adsorption capacity with pH was investigated at 100 µg As/L for an adsorbent dosage of 0.1 g/L. Dilute HCl and NaOH solutions were used to adjust the pH in the range of 4.0-10.0. The final pH was recorded.

The kinetics of adsorption was conducted at pH 6.0 with an adsorbent dose of 0.1 g/L and an As concentration of 100 µg/L by shaking the suspensions at 120 rpm at 25 ± 1 ^{o}C. Samples were taken at different periods (5-300 min), and after filtration of the suspensions, the filtrates were analysed for As using an ICP-MS analyser. The amount of As adsorbed (q_t) at time t was estimated as described below:

$$q_t = \frac{(C_0 - C_t)V}{m} \quad [5]$$

where C_0 is initial concentration of As (µg /L), C_t is concentration of As at time t (µg /L), V is the volume of the solution (L) and m is mass of dry adsorbent (g). The data was modelled using pseudo-first order, pseudo-second order, and Weber and Morris (1963) equations (equations 6, 7, and 8, respectively).

$$\frac{dq_t}{dt} = k_1(q_e - q_t) \quad [6]$$

where q_e = amount of As adsorbed at equilibrium (µg/g), q_t = amount of As adsorbed at time t (h), (µg/g), and k_1 = rate constant for pseudo-first order adsorption (1/h).

$$\frac{dq_t}{dt} = k_2(q_e - q_t)^2 \quad [7]$$

where k_2 = rate constant for pseudo-second order adsorption (g/µg.h).

$$q_t = K_p t^{1/2} + B \quad [8]$$

where k_p = intra-particle diffusion rate constant (µg/(g.h$^{1/2}$)) and B = constant which provides a measure of the boundary layer thickness (µg/g).

2.6. Column experiments

Column studies were conducted in 2 cm diameter glass tubes containing 32 g adsorbents to a height of 30 cm. Solutions containing 100, 250 or 500 µg As/L were passed through the column in the up-flow mode at a velocity of 2.5 or 5 m/h (10.8 or 21.5 mL/min) using a peristaltic pump at 25 ± 1 ^{o}C. The outflow samples were collected at different time intervals and analysed for As concentration.

3. Results and discussion

3.1. Characteristics of GAC adsorbents

The Fe content of the GAC-Fe was 26.1 ± 4.8 mg/g (2.6 ± 0.5%). The surface area, pore volume and pore diameter of the GAC and GAC-Fe are presented in Table 1. The decrease in surface area and pore volume of the GAC after Fe incorporation may be due to blockage of some pores in GAC caused by the iron oxide coating. Others have also reported a reduction in surface area, pore volume and pore size after impregnation of GAC with Fe (Liu et al. 2012) and Fe and Mn (Ryu et al. 2017). This was explained as being due to Fe occupying and blocking some of the internal pores of GAC. The scanning electron micrographs of GAC and GAC-Fe revealed the presence of a large number of pores (Fig. 1) which may have resulted in materials having a high surface area. The presence of Fe oxide aggregates inside some of the pores can be seen in the GAC-Fe micrograph.

Table 1.

Mean (± standard error) values for BET surface area (S_{BET}), pore volume (V_p) and average pore diameter of GAC and GAC-Fe samples.

Sample	S_{BET} (m^2/g)	V_p (cm^3/g)	D_p (nm)
GAC	1124 ± 37	0.62 ± 0.01	2.7 ± 0.1
GAC-Fe	876 ± 77	0.60 ± 0.05	2.8 ± 0.1

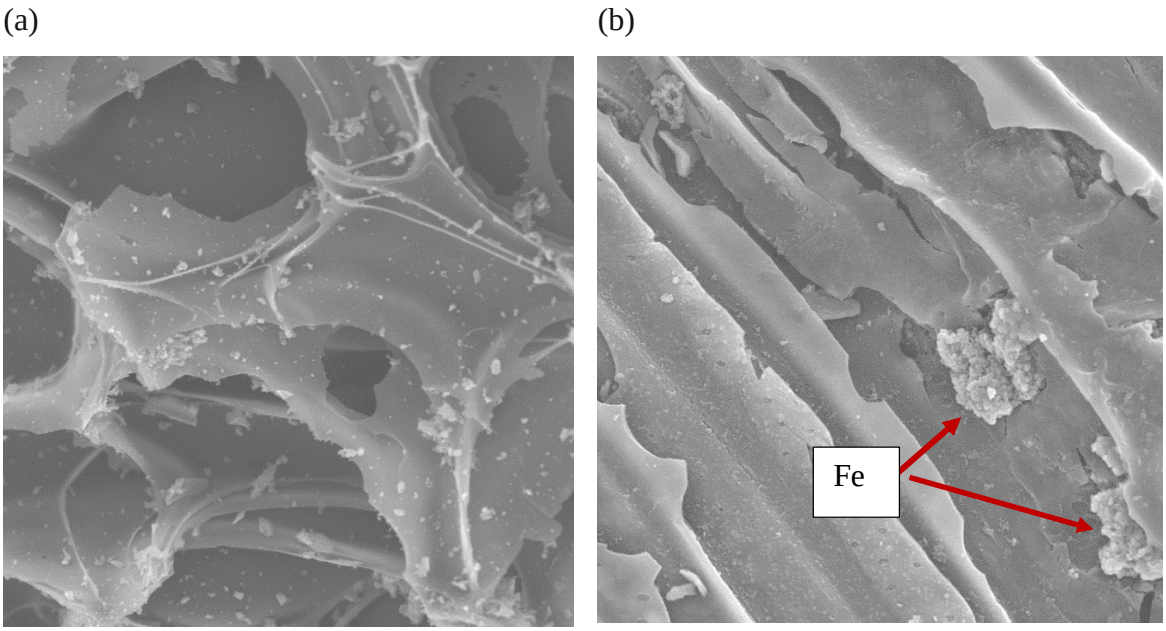

Fig. 1. SEM photos of (a) GAC and (b) GAC-Fe (20 kV x 500 SE). The white square with Fe label inside the right-hand side figure points to the clusters of Fe oxide/hydroxide precipitate that formed on the GAC surface.

3.2. pH effect on zeta potential and As adsorption

The increase in pH decreased the zeta potential of GAC and GAC-Fe, indicating that the negative surface charges on the adsorbents increased with pH (Fig. 2). This suggests that

the adsorption of the negatively charged As ($H_2AsO_4^-$ and $HAsO_4^{2-}$) on these materials would decrease with an increase in pH due to electrostatic repulsion if electrostatic forces govern the adsorption mechanism. When the GAC was modified with Fe (GAC-Fe), the zeta potential increased and became positive up to pH 8. The zero point of charge pH (ZPC) (pH at which the net surface charge is zero) also rose from pH 3.2 to pH 8.0. This suggests that the Fe has provided some positive charges onto the GAC surface and hence the As adsorption capacity was higher for GAC-Fe than for GAC (Fig. 3).

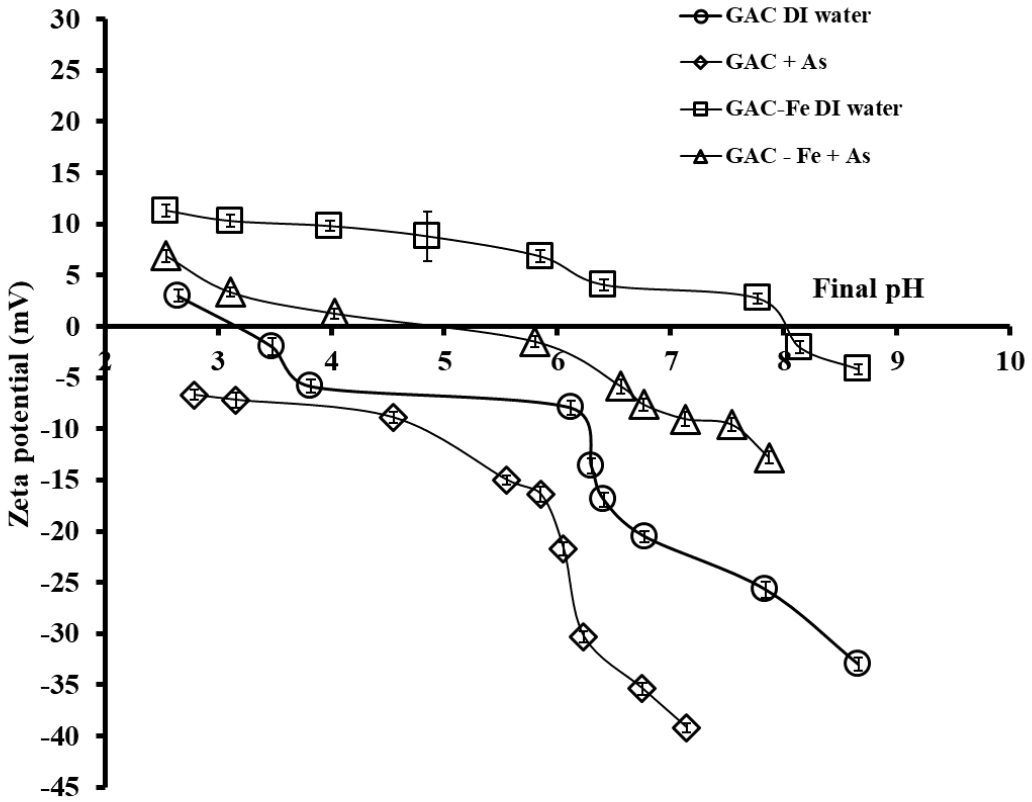

Fig. 2. The pH effect on the zeta potential of GAC and GAC-Fe in deionised (DI) water and As solution (GAC dose 1.0 g/L, ionic strength 10^{-3} M $NaNO_3$, As concentration 100 µg/L). Vertical bars represent standard errors of mean zeta potential values.

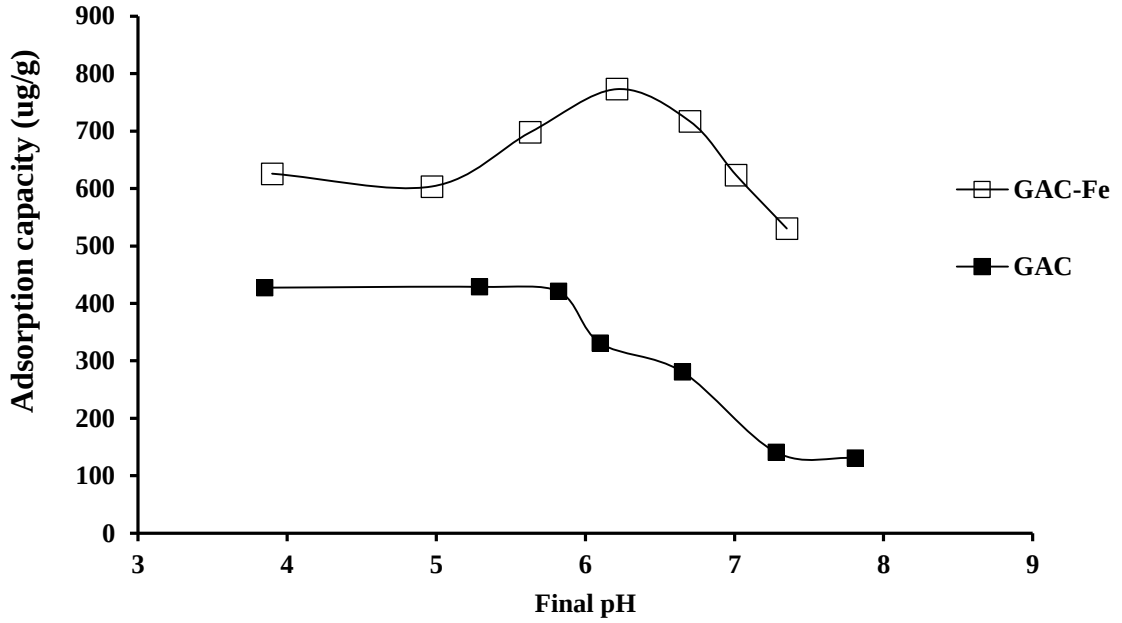

Fig. 3. The pH effects on As adsorption by GAC and GAC-Fe (Adsorbent dose 0.1 g/L, initial As concentration 100 µg/L).

The zeta potential decreased (became more negative) when As was added to GAC and GAC-Fe (Fig. 2), indicating that As was adsorbed by inner-sphere complexation (chemical adsorption) in addition to outer-sphere complexation (electrostatic attraction). Above pH 6.0, As adsorption declined due to increased negative charges on the two adsorbents and on As species (increased concentration ratio of $HAsO_4^{2-}$/ $H_2AsO_4^-$). Furthermore, competition between increased concentrations of OH^- and negatively charged As species ($H_2AsO_4^-$ and $HAsO_4^{2-}$) for adsorption occurred (Liu et al. 2012, Velazquez-Jimenez et al. 2018). The final pH of the suspensions was lower than the initial pH at final pHs greater than pH 6, but the change in pH was negligible at pHs lower than 6. This trend has also been observed by Liu et al. (2012) for Fe-modified bamboo charcoal. The lower final pH is due to the adsorbent releasing H^+ as well as adsorption of OH^- on the adsorbent at high pHs. Another reason for this is that Na added in NaOH for pH alteration might have exchanged with the H ions adsorbed to the adsorbents (Nur et al. 2014).

3.3. Equilibrium batch As adsorption

Equilibrium As adsorption isotherms for GAC and GAC-Fe are presented in Fig. 4. The data is satisfactorily described by both Langmuir and Freundlich adsorption models. However, the Freundlich adsorption model fit was better for both GAC and GAC-Fe with coefficient of determination (R^2) values of 0.94 and 0.99, respectively (Table 2). This means that this model explained 94% and 99% of the variation of the data with correlation coefficients (square root of coefficient of determination) of 0.97 and 1.00, respectively (Little and Hills 1978). These correlation coefficient values are very highly significant for the 9 observation data points (degrees of freedom 8) in the experiment. However, the fit to the Langmuir adsorption model was very satisfactory only for GAC (R^2 = 0.96). The data deviated slightly from this model at high equilibrium As concentrations for GAC-Fe and hence the model fit was slightly poor (R^2 = 0.87). This deviation is probably due to more than one type of adsorption site in GAC-Fe. Perhaps the GAC component provided one type of adsorption site and Fe oxide component another type. Since the Langmuir adsorption isotherm assumes that the adsorption sites are homogeneous, this model explained the adsorption behaviour of GAC-Fe only partially. However, the Freundlich model which is based on heterogeneous adsorption sites was able to explain the data very well (R^2 = 0.99). The Langmuir adsorption capacities for GAC and GAC-Fe were 1.01 and 1.43 mg/g, respectively (Table 2). The Freundlich K_F parameter which is related to the adsorption capacity was also higher for GAC-Fe, confirming that the Fe modification did increase the adsorption capacity of GAC.

In the Langmuir model, the separation factor, R_L is estimated from the equation, $R_L = 1/(1 + C_m K_L)$, where C_m is the maximum initial concentration of adsorbate. The value of R_L indicates the favourability of the adsorption process, i.e. unfavourable ($R_L > 1$), favourable ($0 < R_L < 1$) or irreversible ($R_L = 0$) (Rusmin et al. 2015). The

calculated R_L value for the adsorption of As on GAC was 0.24 and on GAC-Fe it was 0.53. These values suggest that the adsorption process is favourable. The values of the Freundlich constant 1/n were between 0.1 and 1, which also indicated favourable adsorption and implying a stronger interaction between the adsorbents and As (Rusmin et al. 2015).

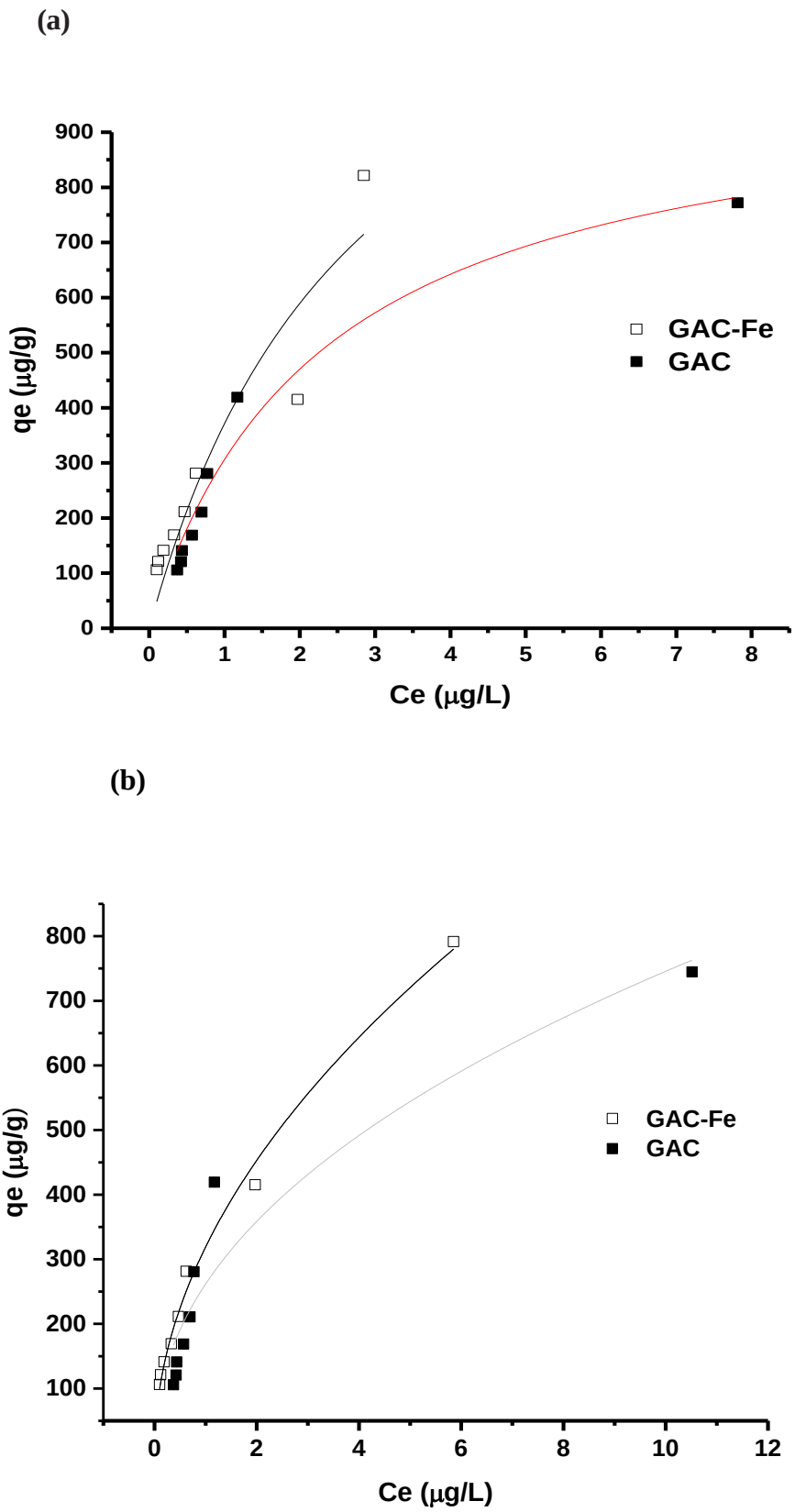

Fig. 4. Batch equilibrium data for As adsorption on GAC and GAC-Fe at pH 6 and the fits of the data points (□, ■) to (a) Langmuir and (b) Freundlich models (curved lines).

Table 2.

Langmuir and Freundlich model parameters and coefficient of determination (R^2) of the models' fits for As adsorption on GAC and GAC-Fe at pH 6.

	Langmuir model			Freundlich model		
Adsorbents	q_m (µg/g)	K_L (L/µg)	R^2	K_F $(µg/g)(L/µg)^{1/n}$	n	R^2
GAC	1013	0.434	0.96	262	2.20	0.94
GAC-Fe	1430	0.351	0.87	319	1.98	0.99

Other researchers have also found that As adsorption capacity of GAC increased markedly when GAC was incorporated with Fe. Gu et al. (2005) reported that the Langmuir adsorption capacity of a Fe-incorporated GAC was 2960 µg/g compared to 38 µg/g for the untreated GAC. Similarly, Yao et al. (2014) showed that the Langmuir adsorption capacity of activated carbon for As increased from 17,860 µg/g to 20,240 µg/g when the activated carbon was modified by incorporation of Fe oxide. The very high adsorption capacities are likely to be due to the exceptionally high equilibrium As concentrations in solution of up to 150,000 µg/L. Gu et al. (2005) reported that the As adsorption capacity of Fe impregnated GAC varied with the type of GAC and the Fe content. They observed that the adsorption capacity increased with Fe content up to 6% but decreased with a further increase in Fe content due to Fe blocking the pores of GAC.

The As adsorption capacity of Fe incorporated GAC (1430 µg/g) observed in the present study is higher than that of many other low-cost adsorbents, such as Fe oxide coated sand and ferrihydrite which had adsorption capacities of 18 µg/g and 285 µg/g, respectively (Thirunavukkarasu et al. 2001). It is also higher than the As adsorption capacities of many natural minerals and waste materials used as adsorbents for As: hematite (219 µg/g) and

feldspar (208 µg/g) (Singh et al. 1996); red mud (510 µg/g) (Altundogan et al. 2002); and chitosan (730 µg/g) (Gerente et al. 2010).

The high As adsorption capacity of GAC-Fe is due to the specific adsorption (inner-sphere complexation) of $H_2AsO_4^-$ and $HAsO_4^{2-}$, the predominant As(V) species at the pH of the experiments (pH 6) (Nguyen et al. 2014), onto GAC-Fe. Gallios et al. (2017) using FTIR spectroscopy showed that the possible mechanism of this adsorption was the substitution of the OH ligand of the Fe (oxyhydr)oxides on the GAC with the As(V) species as described below (Mohan and Pittman 2007):

$$-FeOH + As(V)^- \rightarrow -FeAs(V) + OH^- \quad [9]$$

$$-FeOH + As(V)^{2-} \rightarrow -FeAs(V)^- + OH^- \quad [10]$$

where $As(V)^-$ and $As(V)^{2-}$ represent $H_2AsO_4^-$ and $HAsO_4^{2-}$, respectively. Tuna et al. (2013) reported that the main As(V) adsorption mechanism could occur through complex formation by Lewis acid-base reaction where the As species act as an electron donor and the FeOH group acts as an electron acceptor to form the complex.

The positive zeta potential (Fig. 2) of the GAC-Fe at pH 6 would also have helped the adsorption of the negatively charged As(V) species by electrostatic forces (outer-sphere complexation) (Tuna et al. 2013). Despite the untreated GAC having a negative zeta potential, it adsorbed As, though the adsorption capacity was lower. The adsorption of As by the untreated GAC is possibly due to the high ash content of 6%, which consists of mineral materials (metals and metal oxides) (Lorenzen et al. 1995). The mineral materials are expected to adsorb As. Lorenzen et al. (1995) reported increased As adsorption with an increased ash content of GAC.

3.4. Kinetics of batch As adsorption

Initially, the adsorption of As on both the adsorbents was rapid. Fifty percent adsorption occurred within 30 mins, and this reached 90% in 4-5 h. The data fitted satisfactorily to both the pseudo-first and -second order models (R^2 = 0.92-0.95, Table 3), with the models explaining 92% - 95% of the variation of data. However, the experimental maximum equilibrium adsorption capacity was closer to the predicted adsorption capacity of the pseudo-first order model than the pseudo-second order model for GAC and the opposite case for GAC-Fe. This suggests that the pseudo-first order model is a better predictive model for the adsorption of As on GAC and the pseudo-second order model for the GAC-Fe. It is suggested here that the adsorption mechanism was mostly physical in the case of GAC and chemical for GAC-Fe.

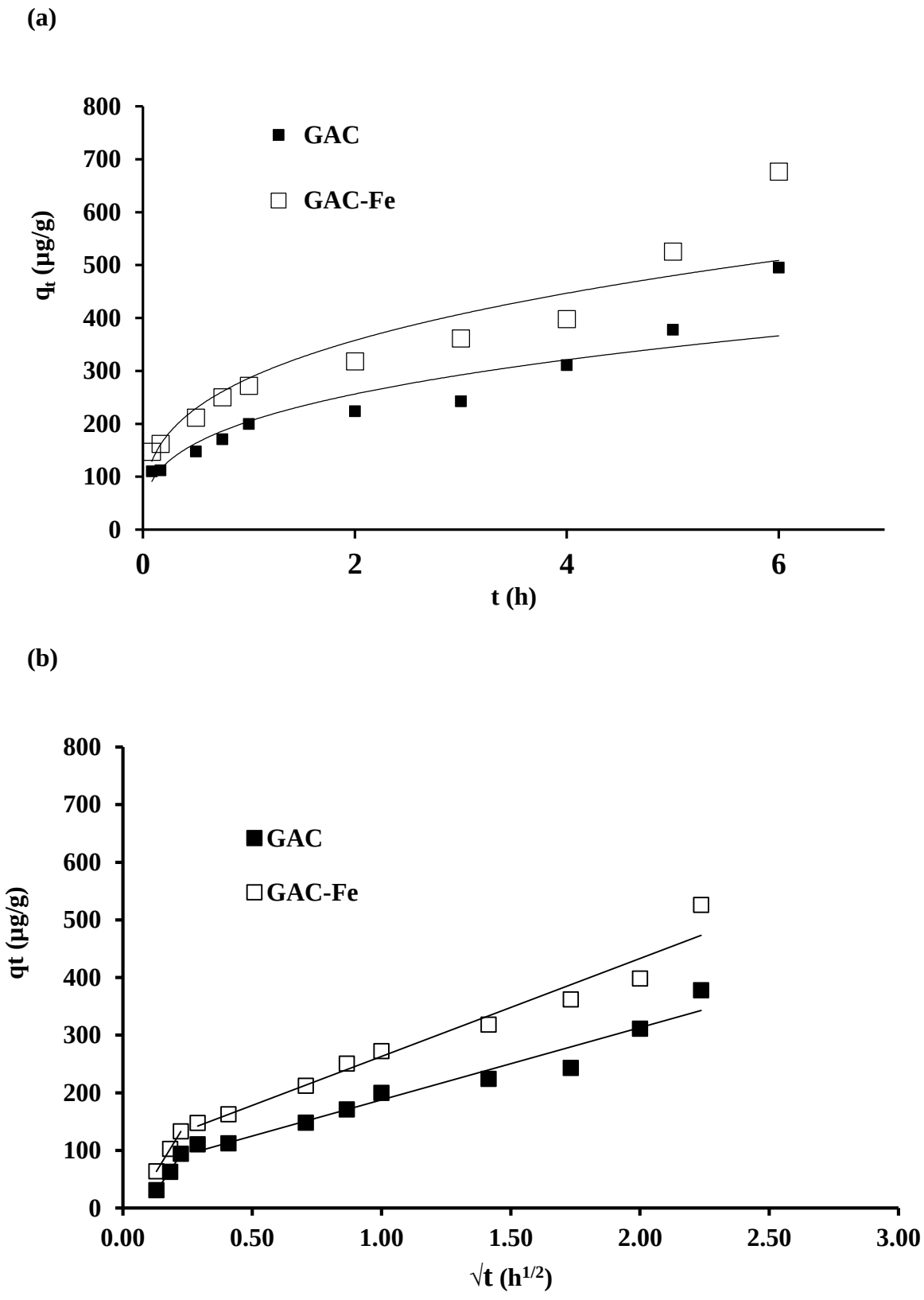

Fig. 5. (a) Batch kinetic data for As adsorption on GAC and GAC-Fe and **(b)** Weber and Morris model fits to the data (pH 6.0, adsorbent dose 0.1 g/L, initial As concentration 100 µg/L)

Table 3.

Batch kinetic model parameter values and coefficient of determinations (R^2) of models fits to data for the adsorption of As on GAC and GAC-Fe at pH 6.0 (adsorbent dose 0.1 g/L, initial As concentration of 100 µg/L).

	Pseudo-first order (PFO)			Pseudo-second order (PSO)				Weber and Morris short-term adsorption		Weber and Morris long-term adsorption	
Adsorbent	q_m µg/g	k_1 h^{-1}	R^2	q_m µg/g	k_2 g/µg h	R^2	qe exp µg/g	Kp_1 µg/(g $min^{1/2}$)	R^2	Kp_2 µg/(g $min^{1/2}$)	R^2
GAC	460	0.16	0.95	370	0.0037	0.92	567	86	1.00	16	0.95
GAC-Fe	556	0.19	0.92	714	0.0005	0.93	707	94	0.99	22	0.96

Since the GAC has pores and channels, the rate of adsorption might have been controlled by As diffusion into these pores and channels. To understand this phenomenon, the kinetic data were fitted to the Weber and Morris model (equation 8) (Weber and Morris 1963). The fit of the data showed two distinct sets of straight lines with high R^2 values of nearly 1.00 for the first set of lines and approximately 0.95 for the second set of lines (Fig. 5, Table 3). The straight-line relationships and the initial line going through the origin in the graph show that the rate of adsorption is controlled by intra-particle diffusion. The rate constant K_p calculated from the two sets of lines (K_{p1} and K_{p2}) indicated an initial fast rate of adsorption followed by a slower rate of adsorption (Table 3). The faster rate of adsorption is probably due to intra-particle diffusion of As into the mesopores of GAC, and the slower rate is due to intra-particle diffusion into the micropores. The rate constants were lower for GAC-Fe than for GAC due to partial blockage of the pores by the Fe oxide coating of GAC.

3.5. Column adsorption of As

The breakthrough curves from the column experiments for As adsorption on GAC and GAC- Fe at the flow velocities of 2.5 and 5.0 m/h and influent As concentrations of 100, 250 and 500 µg/L are presented for different operation times in Fig. 6. The variability in the results, especially at the low As concentrations, is probably due to the very low concentrations used in the experiments. The bed volumes for different times of breakthrough were calculated from the formula, bed volume = flow velocity (m/h) x time of breakthrough (h)/bed height (0.30 m). Results showed that the bed volumes of water treated by GAC-Fe to maintain the As concentration to less than the WHO guideline concentration (10 µg/L) were 4 and 2 times higher (longer operation times) than those treated by GAC for the influent As concentrations of 100 µg/L at 2.5 and 5 m/h flow velocities, respectively (Table 4). The

higher volumes of water treated by GAC-Fe are due to its higher As adsorption capacity (Table 2). The bed volumes of water treated by GAC-Fe were higher for the lower flow velocity because of the longer retention time of As with this adsorbent.

At a lower flow velocity, As had more time to make contact with the adsorbents, which allowed the diffusion of the As ions into the pores of the adsorbent, resulting in a higher proportion of the influent As in the column (lower Ct/ Co) being removed. The column As adsorption capacities are lower than the batch adsorption capacities (Table 2) because in batch experiments, adsorption reached equilibrium and the Langmuir model predicted the maximum adsorption capacity at higher solution As concentration. This was very different from the column experiment, where the adsorption capacities were measured at lower concentrations and adsorption did not reach equilibrium. One concern about the GAC-Fe adsorbent is that the incorporated Fe may leach out of the adsorbent over time and this may reduce its adsorption capacity. This needs to be tested in future studies.

Table 4.

Bed volumes treated by GAC and GAC-Fe columns (2 cm diameter glass tubes containing 32 g adsorbents to a height of 30 cm) to reduce the As concentration to the WHO guideline concentration (10 µg/L) and amount of As adsorbed onto GAC and GAC-Fe

Filtration velocity (m/h)	Adsorbent	As concentration (µg/L)	Bed volume	As adsorption capacity (µg/g)
2.5	GAC	100	388	118
	GAC-Fe	250	784	470
5.0	GAC	100	380	133
	GAC-Fe	100	892	306
	GAC-Fe	250	528	305
	GAC-Fe	500	313	330

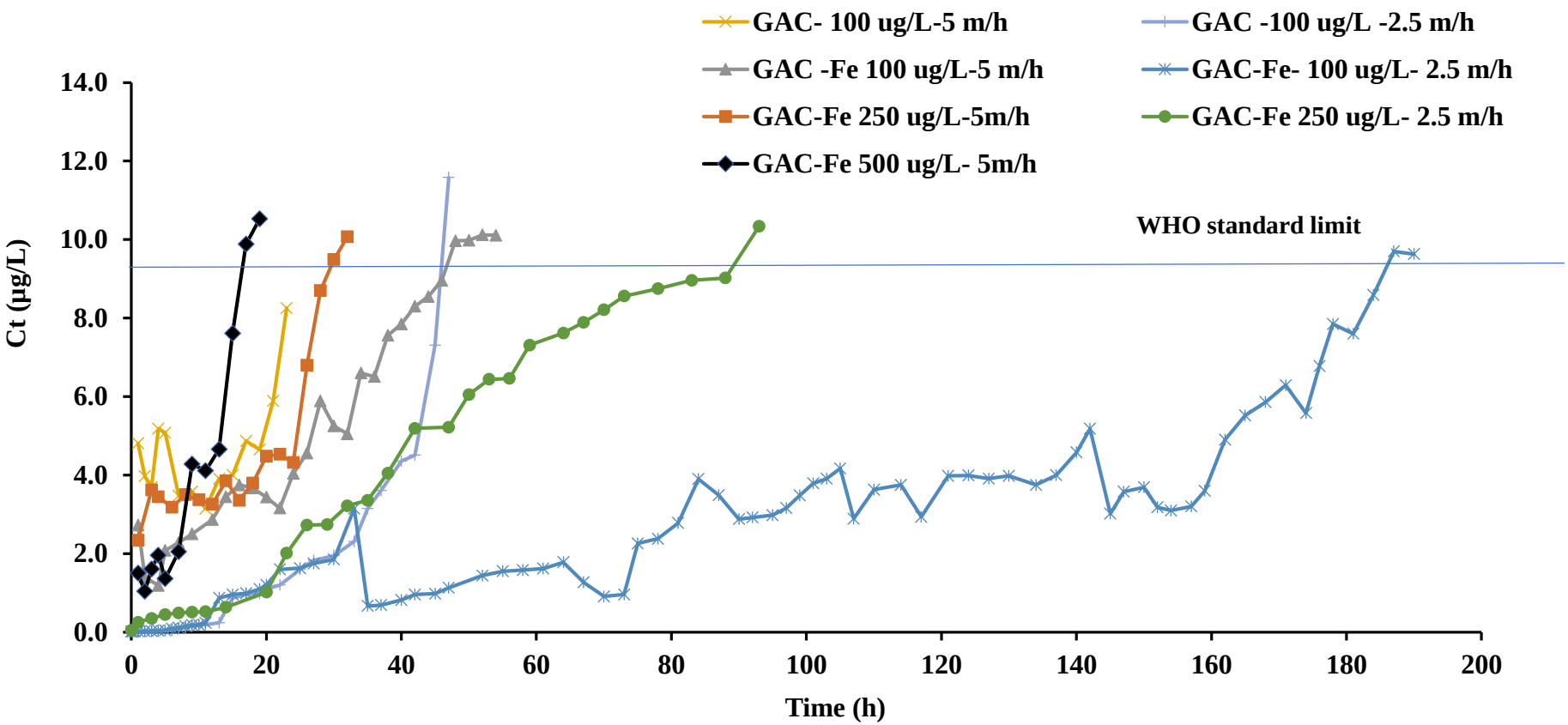

Fig. 6. Breakthrough curves for As adsorption onto GAC and GAC- Fe columns (2 cm diameter glass tubes containing 32 g adsorbents to a height of 30 cm) at different flow rates and influent As concentrations.

3.6. Practical benefits of GAC-Fe column filters

Berg et al. (2006) compared the removal of As from household groundwater and tube wells in Vietnam where the As and Fe concentrations were 10-382 µg/L and 0.1-48 mg/L, respectively, by sand filtration and co-precipitation methods. They reported that As removal rates by co-precipitation were very similar to those of sand filtration and the concentration of dissolved Fe in groundwater was the main factor influencing As removal by co-precipitation. Fe/As ratio > 50 was required for decreasing the As concentration to < 50 µg/L and ratio > 250 to decrease the As concentration to < 10 µg/L. In a study on synthetic water, Hering et al. (1996) reported that a Fe/As ratio of approximately 25 was required to reduce the As concentration from 20 µg/L to 10 µg/L. In another study on synthetic water, Mamtaz and Bache (2001) found that the minimum Fe concentration required to reduce the As level to the Bangladesh standard limit of 50 µg/L by co-precipitation increased exponentially with the As concentration in water. These studies indicate that a high concentration of Fe is required for the removal of As by co-precipitation.

Irrespective of the Fe concentration in water, adsorption onto GAC-Fe beds may be a more suitable method to reduce the As concentration than co-precipitation. Furthermore, the adsorption process is more suitable for practical application because it is easy to operate and manageable. Also, it takes less time for the treatment operation (Berg et al. 2006), production of cleaner water, and has safer As disposal potential. GAC-Fe filters have an advantage over the currently used sand filters in that they are more efficient in adsorbing As, which results in increased amounts of adsorption of both As and Fe as well as organic pollutants. Although sand filtration is generally found to remove a large percentage of As, the As concentration in

many of the treated waters remained higher than the WHO standard (Nguyen et al. 2009), thus requiring further treatment.

4. Conclusions

Batch adsorption studies showed that incorporating Fe into GAC (GAC-Fe) can increase the removal capacity of As(V) from the water. The Langmuir adsorption model fitted the adsorption data for GAC better than that for GAC-Fe. However, the Freundlich adsorption model fitted the data for GAC-Fe better than that for GAC, suggesting the presence of heterogeneous adsorption sites. The higher Langmuir maximum adsorption capacity of GAC-Fe at pH 6 (1430 µg/g) compared to that of GAC (1013 µg/g) is due to inner-sphere complexation of As on Fe oxides in the GAC and outer-sphere complexation on the positive charges created by the Fe oxides. The ZPC of GAC-Fe (pH 8.0) was much higher than that of GAC (pH 3.2). ZPC of pH 8.0 suggested that the GAC-Fe surface was positively charged at pH 6 for favourable adsorption of the negatively charged As. The column adsorption study showed that 2-4 times larger water volumes could be treated by GAC-Fe than by GAC. The volume of water treated increased with a decrease in flow velocity and influent As concentration. As in the batch study, the As adsorption capacity was higher for GAC-Fe (306 µg/g) than for GAC (118-133 µg/g) in the column study for an influent As concentration of 100 µg/L. The advantages of the GAC-Fe filters compared to the currently used sand filters and co-precipitation methods are presented.

Acknowledgement

The Australian Department of Foreign Affairs and Trade (DFAT) via the Google Impact Challenge DFAT Technology Against Poverty (innovation Xchange program) provided the funds for the study. We are grateful to Dr. Andrew Kinsela of the University of New South Wales, Australia, for help in determining surface area, pore size distribution and scanning electron microscopy, and to Mr. Phillip Thomas in Adelaide, South Australia for proof-reading/editing this paper.

References

Altundogan HS, Altundogan S, Tumen F, Bildik M, 2002. Arsenic adsorption from aqueous solutions by activated red mud. Waste Manage. 22: 357-363.

Berg M, Luzi S, Trang PTK, Viet PH, Giger W, Stüben D, 2006. Comparative field study, model calculations, and health benefits. Environ. Sci. Tech. 40: 5567-5573.

Chang Q, Lin W, Ying W, 2010. Preparation of iron-impregnated granular activated carbon for arsenic removal from drinking water. J. Hazard. Mater. 184: 515-522.

Chuang CL, Fan M, Xu M, Brown RC, Sung S, Saha B, Huang BL, 2005. Adsorption of arsenic (V) by activated carbon prepared from oat hulls. Chemosphere 61: 478–483.

Daus B, Wennrich R, Weiss H, 2004. Sorption materials for arsenic removal from water: a comparative study. Water Res. 38: 2948-2954.

Gallios GP, Tolkou AK, Katsoyiannis IA, Stefusova K, Vaclavikova M, Deliyanni EA, 2017. Adsorption of arsenate by nano scaled activated carbon modified by iron and manganese oxides. Sustainability. 9: 1684.

Gerente C, Andres Y, McKay G, Le Cloirec P, 2010. Removal of arsenic (V) onto chitosan: from sorption mechanism explanation to dynamic water treatment process. Chem. Eng. J. 158: 593–598.

Gu Z, Fang J, Deng B, 2005. Preparation and evaluation of GAC-based iron-containing adsorbents for arsenic removal. Environ. Sci. Technol. 39: 3833-3843.

Hering JG, Chen P, Wilkie JA, Elimelech M, Liang S, 1996. Arsenic removal by ferric chloride. Amer. Water Works Assoc. J. 88: 155-167.

Kabir F, Chowdhury S, 2017. Arsenic removal methods for drinking water in the developing countries: technological developments and research needs. Environ. Sci. Pollut. Res. 24: 24102-24120.

Little TM, Hills FJ, 1978. Agricultural Experimentation, Design and Analysis, John Willey and Sons, New York.

Liu X, Ao H, Xiong X, Xiao J, Liu J, 2012. Arsenic removal from water by iron-modified bamboo charcoal. Water Air Soil Pollut. 223: 1033-1044.

Liu Z, Zhang FS, Sasai R, 2010. Arsenate removal from water using Fe_3O_4-loaded activated carbon prepared from waste biomass. Chem. Eng. J. 160: 57–62.

Lodeiro P, Kwan SM, Perez JT, Gonzalez LF, Gerente C, Andres Y, McKay G, 2013. Novel Fe loaded activated carbons with tailored properties for As (V) removal: adsorption study correlated with carbon surface chemistry. Chem. Eng. J. 215: 105–112.

Loganathan P, Vigneswaran S, Kandasamy J, Bolan NS, 2014. Removal and recovery of phosphate from water using sorption. Crit. Rev. Environ. Sci. Technol. 44: 847-907.

Lorenzen L, van Deventer JSJ, Land WM, 1995. Factors affecting the mechanism of the adsorption of arsenic species on activated carbon. Miner. Eng. 8: 557–569.

Luu TL, 2017. Remarks on the current quality of groundwater in Vietnam. Environ. Sci. Pollut. Res. (in press); https://doi.org/10.1007/s11356-017-9631-z.

Mamtaz, R, Bache DH, 2001. Reduction of arsenic in groundwater by coprecipitation with iron. J. Water Supply: Res. Tech. – Aqua 50.5: 313-324.

Manju, GN, Raji C, Anirudhan TS, 1998. Evaluation of coconut husk carbon for the removal of arsenic water. Water Res. 32: 3062-2070.

Meng X, Korfiatis GP, Christodoulatos C, Bang S, 2001. Treatment of arsenic in Bangladesh well water using a household co-precipitation and filtration system. Water Res. 35: 2805-2810.

Mohan D, Pittman CU, 2007. Arsenic removal from water/wastewater using adsorbents – a critical review. J. Hazard. Mater. 142: 1-53.

Mohanty, D, 2017. Conventional as well as emerging arsenic removal technologies—a critical review. Water Air Soil Pollut. 228: 381.

Mondal MK, Garg R, 2017. A comprehensive review on removal of arsenic using activated carbon prepared from easily available waste materials. Environ. Sci. Pollut. Res. 24: 13295-13306.

Natale FD, Erto A, Lancia A, Musmarra D, 2008. Experimental and modelling analysis of As (V) ions adsorption on granular activated carbon. Water Res. 42: 2007–2016.

Nguyen TV, Loganathan P, Vigneswaran S, Krupanidhi S, Nga Pham TT, Ngo H, 2014. Arsenic waste from water treatment systems: characteristics, treatments and its disposal. Water Sci. Treat. Water Supply 14: 939-950.

Nguyen VA, Bang S, Viet PH, Kim K, 2009. Contamination of groundwater and risk assessment for arsenic exposure in Ha Nam province. Vietnam. Env. Inter. 35: 466-472.

Nur T, Loganathan P**,** Nguyen TC, Vigneswaran S, Singh G, Kandasamy J, 2014. Batch and column adsorption and desorption of fluoride using hydrous ferric oxide: Solution chemistry and modelling. Chem. Eng. J. 247: 93-102.

Rusmin R, Sarkar B, Liu Y, McClure S, Naidu R, 2015. Structural evaluation of chitosan-palygorskite composites and removal of aqueous lead by composite beads. Appl. Surf. Sci. 353: 363-375.

Ryu S, Jeon E, Yang J, Baek K, 2017. Adsorption of As(III) and As(V) in groundwater by Fe-Mn binary oxide – impregnated granular activated carbon (IMIGAC). J. Taiwan Inst. Chem. Eng. 72: 62-69.

Singh DB., Prasad G., Rupainwar DC, 1996. Adsorption technique for the treatment of

As(V) rich effluents. Colloid Surf. 111 (1–2): 49–56.

Thirunavukkarasu, OS, Viraraghavan T, Subramanian KS, 2001. Removal of arsenic in drinking water by iron oxide-coated sand and ferrihydrite batch studies. Water Qual. Res. J. Canada 36: 55–70.

Tuna AÖA, Özdemir E, Şimşek EB, Beker U, 2013. Removal of As (V) from aqueous solution by activated carbon–based hybrid adsorbents: impact of experimental conditions. Chem. Eng. J. 223: 116–128.

Velazquez-Jimenez LH, Arcibar-Orozco JA, Rangel-Mendez JR, 2018. Overview of As(V) adsorption on Zr-functionalized activated carbon for aqueous streams remediation. J. Environ. Manage. 212: 121-130.

Weber WJ, Morris JC, 1963. Kinetics of adsorption on carbon from solution. J. Sanit. Eng. Div. - ASCE 89:31-59.

Yao S, Liu Z, Shi Z, 2014. Arsenic removal from aqueous solutions by adsorption onto iron oxide/activated carbon magnetic composite. J. Environ. Health Sci. Eng. 12: 58.